# INFLUENCE OF LOADING FREQUENCY ON THE ELEVATED TEMPERATURE FATIGUE BEHAVIOR OF FIBER-REINFORCED CERAMIC COMPOSITES

Report for the period 10-1-97 to 9-30-98
Contract # F49620-98-1-0018

John W. Holmes
Principle Investigator
Department of Mechanical Engineering and Applied Mechanics


Ceramic Composites Research Laboratory
The University of Michigan
Ann Arbor, MI 48109

Submitted to

20000526 006

# REPORT DOCUMENTATION PAGE

AFRL-SR-BL-TR-00-

*0187*

id reviewing
Information

| 1. AGENCY USE ONLY *(Leave blank)* | 2. REPORT DATE | 3. REPORT TYPE AND DATES COVERED |
|---|---|---|
| | January 15, 1999 | FINAL TECHNICAL REPORT  1 Oct 97 - 30 Sep 99 |

**4. TITLE AND SUBTITLE**
EFFECT OF LOADING MODE ON ELEVATED TEMPERATURE FATIGUE
DAMAGE IN CERAMIC MATRIX COMPOSITES

**5. FUNDING NUMBERS**
F49620-98-1-0018

61102F
2306/BS

**6. AUTHOR(S)**
JOHN W. HOLMES

**7. PERFORMING ORGANIZATION NAME(S) AND ADDRESS(ES)**
UNIVERSITY OF MICHIGAN
DEPT OF MECHANICAL ENGINEERING AND APPLIED MECHANICS
CERAMIC COMPOSITES RESEARCH LABORATORY
ANN ARBOR MI  48109

**8. PERFORMING ORGANIZATION
REPORT NUMBER**

**9. SPONSORING/MONITORING AGENCY NAME(S) AND ADDRESS(ES)**
AIR FORCE OFFICE OF SCIENTIFIC RESEARCH
801 N. RANDOLPH STREET, ROOM 732
ARLINGTON, VA  22203-1977

**10. SPONSORING/MONITORING
AGENCY REPORT NUMBER**

**11. SUPPLEMENTARY NOTES**

**12a. DISTRIBUTION AVAILABILITY STATEMENT**
APPROVED FOR PUBLIC RELEASE, DISTRIBUTION IS UNLIMITED

**12b. DISTRIBUTION CODE**

**13. ABSTRACT** *(Maximum 200 words)*
Cyclic tension-tension experiments were conducted on a ceramic matrix     composite of continuous Nicalon SiC-fibers in a calcium-aluminosilicate     matrix. Two different stress ratios ($R = \sigma_{min}/\sigma_{max}$) were studied ($R = 0.5$ and $R = 0.05$) at a loading frequency of 200 Hz. Specimens tested at $R = 0.05$   were found to have a shorter fatigue life than specimens tested at $R = 0.5$.   The fatigue limit (defined as run-out at $10^8$ cycles) increased from 212 MPa for $R = 0.05$ to 240 MPa for $R = 0.5$. Microstructural investigations revealed  an internal zone with no fiber pull-out at the fracture surface, suggesting  that the fatigue failures occur due to internal embrittlement. The loading   condition with smallest stress range (i.e., the largest stress ratio) has the lowest amount of interfacial sliding (and thus the lowest frictional energy  dissipation). It is therefore plausible that the fatigue damage is related to the amount of interfacial sliding.

| 14. SUBJECT TERMS | | 15. NUMBER OF PAGES |
|---|---|---|
| | | 31 |
| | | **16. PRICE CODE** |

| 17. SECURITY CLASSIFICATION OF REPORT | 18. SECURITY CLASSIFICATION OF THIS PAGE | 19. SECURITY CLASSIFICATION OF ABSTRACT | 20. LIMITATION OF ABSTRACT |
|---|---|---|---|
| U | U | U | |

# Influence of Stress Ratio on the Fatigue Life of a Silicon-Carbide Fiber Reinforced Ceramic Matrix Composite

Abstract

Cyclic tension-tension experiments were conducted on a ceramic matrix composite of continuous Nicalon SiC-fibers in a calcium-aluminosilicate matrix. Two different stress ratios ($R = \sigma_{min}/\sigma_{max}$) were studied ($R = 0.5$ and $R = 0.05$) at a loading frequency of 200 Hz. Specimens tested at $R = 0.05$ were found to have a shorter fatigue life than specimens tested at $R = 0.5$. The fatigue limit (defined as run-out at $10^8$ cycles) increased from 212 MPa for $R = 0.05$ to 240 MPa for $R = 0.5$. Microstructural investigations revealed an internal zone with no fiber pull-out at the fracture surface, suggesting that the fatigue failures occur due to internal embrittlement. The loading condition with smallest stress range (i.e., the largest stress ratio) has the lowest amount of interfacial sliding (and thus the lowest

1

frictional energy dissipation).  It is therefore plausible that the fatigue damage is related to the amount of interfacial sliding.

## I.    Introduction

Continuous fiber reinforced ceramic matrix composites (CMCs) posses a unique combination of damage tolerant behavior and high temperature stability.  This feature makes CMCs promising candidates for load carrying structures at high temperature. Most applications, such as turbine blades or heat exchangers, involve changes in the applied load.  Thus, components must be designed against mechanical fatigue.

Earlier studies of mechanical fatigue of fiber reinforced CMCs [1,2,3] have shown that a true fatigue limit, $\sigma_{fl}$, (defined by the maximum cyclic stress that the material can sustain for an infinite number of load cycles) can, in principle, only exist if cyclic slip (along the fiber / matrix interface) is avoided.  These conditions are only present at exceedingly low applied stresses. However, in a practical sense, an engineering definition for the fatigue limit can be specified at an arbitrary number of cycles.

For CMCs with weakly bonded fiber-matrix interfaces the basic picture of the fatigue damage evolution process is as follows.  Multiple matrix cracks form in the early stages of cycling.  In parallel, fiber-matrix debonding and sliding take place, such that intake

2

fibers bridge the matrix cracks. This results in changes in the macroscopic properties; the cyclic stress-strain relationship exhibits hysteresis, the hysteresis modulus decreases, and a permanent strain develops. On a microscale, repeated forward and reverse interfacial sliding causes wear of interfacial roughness, which decreases the interfacial frictional shear stress. This may reduce the composite strength and can contribute to fatigue failure [4]. Experimental studies indicate that wear of interfacial asperities occurs within a relative low number of cycles [5]. On a cycle basis, fatigue failure usually occurs much later than the decrease in the interfacial shear stress [6]. One possible explanation is wear damage of the fibers, induced by cyclic sliding along the fiber-matrix interface and for woven composites, at the cross-over points of fiber bundles [7]. Direct wear damage has been observed in composites with soft carbon fibers [8]. Other strength degrading mechanisms, such as stress corrosion and oxidation damage to the fiber / matrix interfaces or the fibers, may also affect the strength of composite during long term cyclic loading [9,10,11,12,13].

For the fatigue of composites which exhibit fiber-matrix sliding, one would expect that the rate of microstructural damage evolution would depend upon the stress range, $\Delta\sigma = \sigma_{max} - \sigma_{min}$, as follows. If the stress range is increased, a higher wear rate would be expected (the relative sliding velocity and sliding displacement between fibers and matrix would increase), resulting in a more rapid decrease in the interface shear stress and an increasing rate of wear damage to the fibers. A higher stress range also increases energy dissipation, and thus the local temperature along the interface – accelerating the rate and degree of possible interfacial oxidation.

In the literature, there are very few studies that address the effect of stress ratio on fatigue damage evolution. Moschelle [14] conducted room temperature fatigue experiments at R-ratios (R = $\sigma_{min}/\sigma_{max}$) of 0.1 and −1.0 in woven SiC/SiC composites. It was found that the fatigue life of specimens subjected to R = -1.0 was shorter than the ones cycled with an R-ration of 0.1. Holmes [15] studied the effect of R-ratio on SiC/Si$_3$N$_4$ composites at 1200°C. The fatigue life for R = 0.1 was shorter than for R = 0.3, which again was shorter than for R = 0.5. The fatigue limit (run-out defined at 5 X 10$^6$ cycles at 10 Hz) was similar for all R-ratios.

The purpose of the present paper is to study the relationship between the applied stress ratio and the damage evolution, frictional heating and fatigue life of CMCs. This is accomplished by conducting cyclic tension-tension tests for two stress ratios (R = 0.05 and R = 0.5) and using an analytical micromechanical model to interpret the experimental results.

II. **Experimental Program**

A 16-ply unidirectional SiC-fiber reinforced calcium-aluminosilicate matrix composite (SiC$_f$/CAS II, Corning, Inc., NY) was used in the fatigue experiments. The composite was supplied as hot pressed plates (160 mm by 150 mm). Edge loaded tensile specimens (Fig. 1), with the tension directed parallel to the fiber direction, were machined from the

4

plates using diamond tooling. A minor face of each specimen was polished to allow observation of matrix cracks. The polishing was performed using a 38 mm mandrel rotating at 1500 rpm. The following polishing procedure was used: (1) 600 grit SiC paper for 5 min., (2) 45 $\mu$m diamond paste for 5 min. (nylon cloth), (3) 6 $\mu$m diamond paste for 5 min. (nylon cloth), (4) 1.0 $\mu$m diamond paste for 10 min. (nylon cloth).

Fatigue tests were conducted on a MTS servo-hydraulic load frame (Model 331, MTS Systems Corporation, Minneapolis, MN). Specimens were cycled under load control at a sinusoidal frequency of 200 Hz. The specimen and grips were enclosed in an isothermal chamber; the walls of the chamber were water-cooled to 20 $\pm$ 0.1 $^{\circ}$C (for details of the experimental setup see Holmes and Cho [6]). The surface temperature of the specimens was measured using infrared pyrometers; strain was measured by an extensometer. The specimens were cycled to fatigue failure or $10^8$ cycles (run-out). After cycles, the average matrix crack spacing, s, was calculated by counting the number of matrix cracks along a line (parallel with the fiber direction) that traversed the entire 33 mm length of the gage section. Specimens surviving $10^8$ cycles were tested in monotonic tension (loading rate 100 MPa / s) to assess their residual strength. Finally, the fracture surfaces were inspected in a scanning electron microscope.

III. Experimental Results

The S-N curve, constructed from the experimental data, is shown in Fig. 2 for the two stress ratios examined (R =0.5 and R = 0.05). Several points should be noted. First, an increasing R-ratio resulted in a longer fatigue life. Such a trend has also been found for

5

other CMCs [14,15]. Second, distinct fatigue limits (defined here as run-out for $10^8$ cycles at 200 Hz) exist for both stress ratios. Third, the fatigue limit increased from 212 MPa at R = 0.05 to 240 MPa at R = 0.5.

Table I compares the measured crack spacing, s, of specimens subjected to identical $\sigma_{max}$ but different R-ratios (different $\sigma_{min}$). For identical $\sigma_{max}$, the specimens with the higher $\sigma_{min}$ develop more matrix cracks (lower value of s). Note, that for $\sigma_{max}$ = 220 MPa and $\sigma_{max}$ = 240 MPa (where fatigue failure occurs for R = 0.05 but not for R = 0.5) the *run-out specimens* (R = 0.5) *have developed more matrix cracks than the specimens that failed in fatigue* before $10^6$ cycles. Thus, matrix crack spacing cannot be used as a predictor of fatigue failure.

For the two stress ratios, Fig. 3 shows the evolution of the hysteresis modulus, $\overline{E}$, as a function of the number of cycles, $N$ ($\sigma_{max}$ = 240 MPa). Both specimens experienced a significant modulus decrease. The modulus of the specimen subjected to $R = 0.5$ reached a steady-state value that approximately 2 x $10^6$ cycles. The modulus of the specimens subjected to R = 0.05 decreases also, but the specimen fails before a steady-state value is attained. Note, that the value of $\overline{E}$ immediately prior to failure ($R = 0.05$) is higher than the run-out value at $R = 0.5$. Thus, as with crack spacing, modulus cannot be used as a predictor of fatigue failure.

Figure 4 shows the temperature rise curves for tests conducted at $R = 0.05$ and $R = 0.5$. The temperature rise was largest for the specimen subjected to the largest stress range

6

(smallest R-value), see also Table I. Similar results have been obtained by Cho *et al.* [16].

For specimens that did not fail within $10^8$ cycles, the temperature increased in the early

stages of cycling, reached a maximum, and decreased thereafter. In contrast, nearly all

specimens that failed during cycling failed while the temperature was still rising.

Figure 5 and 6 compares the fracture surfaces of specimens that failed during cycling

with those that survived $10^8$ cycles. The fracture surface of specimens surviving $10^8$

cycles exhibits fiber pull-out across the entire fracture surface. In contrast, all specimens

that failed in fatigue had a large core region, where no fiber pull-out occurred (there was

no apparent difference in the appearance of the fracture surface of specimens failing

under $R = 0.05$ and $R = 0.5$). Since all fibers in the core region have fractured at the same

matrix-crack plane, the failure mechanism must be such that fibers that fail cause

neighboring fibers to fail there too, i.e., there must be *local load sharing*. Consequently,

composite models based on *global load sharing* [4,17] cannot be used to interpret the failure

process. Possible mechanisms for the formation of the core region with negligible fiber

pull-out length are discussed in detail elsewhere [10].

Residual strength data for specimens that survived $10^8$ cycles are also given in Table I.

The residual strength of the run-out specimens is only 5 to 20 % lower than the strength

of the virgin material, which is about 500 MPa. Thus, cycling to $10^8$ cycles at a stress

level below $\sigma_{fl}$ does reduce the composite strength and modulus (indicating that fatigue

damage does develop), but the residual strength is still significantly higher than the

fatigue limit. A typical stress-strain curve from the residual strength tests is shown in

Fig. 7. In contrast to the stress-strain curve for the virgin material, the stress-strain curve

7

of pre-cycled specimens is non-linear even at low stresses. The non-linearity becomes more progressive above approximately 240 MPa (the max. fatigue stress) this non-linearity is attributed to interfacial sliding and (at stresses above 240 MPa) the development of additional matrix cracks and distributed fiber failures (note from Table I that more matrix cracks are present after the residual strength test).

## IV.    Interpretation and Discussion

In the following, we will use a simple analytical model to extract insight from the modulus and temperature rise data. The aim is to obtain information about the interfacial shear stress, $\tau$. The model is based on distributed damage in the form of multiple matrix cracks and interfacial sliding (interfacial debonding is assumed to occur easily). The model is only valid when the amount of fiber fractures are negligible. Within the framework of the model, the damage is described by two parameters, $s$ and $\tau$. Since $s$ can be measured directly, $\tau$ is the only unknown property.

### (1) Linear Elastic Behavior

For the undamaged composite the linear elastic response can be predicted from the rule of mixtures for unidirectional composites.

$$E_c = v_f E_f + (1 - v_f) E_m \tag{1}$$

8

where $v_f$ is the volume fraction of fibers, $E_c$, $E_f$ *and* $E_m$ are the elastic moduli of the composite, fibers and matrix respectively. $E_c$ becomes 134 GPa when the values from Table II (data for fiber and matrix is from Daniels *et al.*[18]) are used. This value is in agreement with experimental findings.

*(2) Calculation of $\tau$ from Cyclic Behavior*

For the damaged composite, different equations must be used for partial slip (i.e., when the maximum cyclic slip zone is less than s/2) and full slip (the cyclic slip zone equals s/2).

The hysteresis modulus, $\overline{E}$ (defined from the stress-strain data of the maximum and minimum applied stress), is not a material constant, since it depends on the applied stress range, $\Delta\sigma$ (see below). However, $\overline{E}$ can be useful means to extract information on the evolution of $\tau$ during cycling. It is convenient to use $\overline{E}$ to distinguish between the state of slip, as follows. The hysteresis modulus under partial slip is [19,20,21]

$$\overline{E_{ps}} = \frac{E_c}{1 + \dfrac{r}{4s}\dfrac{E_c}{\tau}\dfrac{\Delta\sigma}{E_f}\left(\dfrac{1 - v_f}{v_f}\dfrac{E_m}{E_c}\right)^2} \quad , \qquad (2)$$

9

where $r$ is the radius of the fibers. The hysteresis modulus under full slip conditions can be found as [20,21]

$$\overline{E_{fs}} = \frac{v_f E_f}{1 - v_f \dfrac{s}{r} \dfrac{\tau}{\Delta\sigma}}. \qquad (3)$$

Note, that an increase in $\Delta\sigma$ (lower R-ratio for constant $\sigma$ max), always results in a lower hysteresis modulus. The transition between full slip and partial slip occurs at a value given by [21]

$$\overline{E}_{ps-fs} = \frac{E_c}{1 + \dfrac{1 - v_f}{2v_f} \dfrac{E_m}{E_f}}. \qquad (4)$$

This transition modulus is particularly useful, since it is a simple means of determining the state of slip; $\overline{E}_{ps-fs}$ does not depend on stress range and the damage state (s and $\tau$). If the recorded value of $\overline{E}$ is less than $\overline{E}_{ps-fs}$ the composite is in full slip; if $\overline{E}$ is higher than $\overline{E}_{ps-fs}$ the composite is in partial slip.

Using the values given in Table II gives $\overline{E}_{ps-fs} = 91.9$ GPa. The experimental values of $\overline{E}$ (Table I) are larger than $\overline{E}_{ps-fs}$, so that the partial slip equation (2) must be used for the calculation of $\tau$ The calculated values of $\tau$ are about 10 MPa (Table III).

10

The values in parenthesis in Table III were determined from the average modulus of the stress-strain data (0  0.2 % strain), obtained from the residual strength tests. They are comparable to the values obtained during cycling. The computed values are comparable with, but higher than those measured by cyclic experiments by Holmes and Cho [6] and by Evans et al. [5]. The difference may be attributed to differences in processing conditions. Another difficulty is that the equations are sensitive to some of the parameters. For instance, had we used $E_m$ = GPa (as used by Holmes and Cho[6]) instead of the more commonly quoted value of 98 GPa, the rule of mixtures would give us $v_f = 0.42$, and the values of $\tau$ would be reduced by roughly a factor of two (this would result in a value of $\tau$ identical to that calculated by Holmes and Cho[6]). In any case, the values obtained during cycling are lower than the values of $\tau$ in the unfatigued $SiC_f$/CAS II, which has been measured by fiber push out tests to be about 20-30 MPa [6,22] The difference between values obtained in virgin and cycled material has been attributed to wear of interfacial roughness in the early stages of cycling [6,9].

### (3) Evolution of Matrix Crack Spacing

As noted earlier, for identical $\sigma_{max}$, specimens cycled at R= 0.5 show a higher crack density in comparison with those cycled at $R = 0.05$. This can be attributed to stress corrosion cracking, which is a common phenomenon in glass-ceramic matrices, including CAS [23]. The R = 0.5 specimens are subjected to the higher $\sigma_{min}$, and spend more time

11

near $\sigma_{max}$. Consequently, more stress-corrosion-assisted matrix crack growth is expected.

### *(4) Discussion of Failure Mechanism*

The present results (Table III) indicate that $\tau$ decreases during cycling to a value that is roughly the same for all conditions, i.e., independent of $\sigma_{max}$. This is in agreement with the results presented by Evans [24], showing that the decrease in $\tau$ in SiC$_f$/MAS evolved in a similar manner for three different stress ranges.

The fact that specimens failing in high cycle fatigue displayed a fracture surface with an embrittled core region, exhibiting no fiber pull-out, suggests that global load sharing (GLS) does not take place during the final stages of fatigue. Post-fatigue fracture surfaces (of specimens that had survived $10^8$ cycles) displayed significant fiber pull-out. For these specimens then, the GLS models should be applicable.

Denoting $\sigma_u^o$ and $\tau^0$ as the initial values for the overall composite strength and interfacial shear stress, respectively, and $\sigma_u$ and $\tau$ as values occurring during cycling (any possible change in fiber strength is not considered here), GLS models [4,17] predict the following relationship between the ratio of strength and the ratio of $\tau$

12

$$\frac{\sigma_u}{\sigma_u^o} = \left(\frac{\tau}{\tau^0}\right)^{1/(m+1)} \qquad (4)$$

where $m$ is the Weibull modulus describing the strength variation of the fibers. Using a value of $m = 3$ (taken from Curtin[17]) and a reduction in $\tau$ from 30 to 10 MPa (after $10^8$ cycles) predicts a residual strength, $\sigma_u$, of 350 MPa of run-out specimens. The experimental results (Table II) are 16 – 37 % higher than this prediction.

Although the high cycle fatigue mechanism responsible for strength reduction is presently unknown, it is plausible that fatigue damage localization occurs when the temperature *locally at the interface* exceeds a critical value for a certain time period. It is clear from Table I that the maximum temperature *measured at the specimen surface* cannot be used as a simple criterion for whether fatigue failure occurs. However, the temperature field in a tensile specimen heating up due to frictional energy dissipation depends on many parameters, such as specimen geometry and thermal boundary conditions (see Cho *et al.* [16] for a comprehensive discussion and modeling). Dependent on the heat transfer in the transverse direction, the temperature in the middle of the cross section of the specimen may be higher than the surface temperature. Also, the temperature locally at the fiber / matrix asperities may be much higher than the bulk temperature.

## V.    Conclusions

Tension-tension fatigue experiments, conducted on a unidirectional SiC-fiber reinforced calcium-aluminosilicate ceramic matrix composite at 200 Hz, show that room temperature fatigue damage evolution depends strongly on the stress ratio. The results of this work show that:

1.  The fatigue life of specimens cycled at $R = 0.5$ is roughly a factor of ten longer than that of specimens cycled at $R = 0.05$.

2.  The fatigue limit (run-out at $10^8$ cycles) increases from 212 MPa at $R = 0.05$ to 240 MPa at $R = 0.5$.

3.  Initially, the damage evolves rapidly, stabilizes, and accelerates just prior to fatigue failure. But neither the evolution of the temperature rise, hysteresis modulus, or matrix crack spacing can be used to predict if fatigue failure will occur. However, the presence of a temperature rise indicates that cyclic damage on the form of interface slip is occurring.

4.  The fracture surfaces of specimens failing in fatigue posses a central zone with no fiber pull-out, indicating that global load sharing no longer occurs in this zone. This embrittled zone may have formed as a result of internal heating.

**Figures**

1)  Geometry of the edge loaded tensile specimens used in the present study.

2)	The S-N curve (relationship between the maximum applied stress and the number of cycles to failure) for $R = 0.05$ and $R = 0.5$. Both fatigue life and the fatigue limit (defined as run-out for $10^8$ cycles) increases with increasing stress ratio ($\sigma_{max} = 240$ MPa).

3)	Hysteresis modulus as a number of cycles for two specimens loaded with identical maximum stress (240 MPa) at two stress ratios ($R = 0.05$ and $R = 0.5$).

4)	The evolution of temperature rise of cyclically loaded specimens. The maximum stress is identical for the two specimens (240 MPa), but their stress ratios are different ($R = 0.05$ and $R = 0.5$)

5)	Micrographs of fracture surface of a specimen failing in fatigue. (a) overview of fracture surface, (b) the transition zone between the central zone with (right) and without fiber pull out (left), (c) close up of the central part of the fracture surface.

6)	Micrographs of fracture surface of a specimen that survived $10^8$ cycles. (a) overview, (b) close up of the central part of the fracture surface.

7)	A typical stress-strain curve of a specimen after $10^8$ load cycles.

**Tables**

## Table I: Minimum hysteresis modulus, maximum temperature rise and average matrix crack spacing measured after cyclic loading at 200 Hz.

### R=0.05

| $\sigma_{max}$ (MPa) | $\overline{E}_{min}$ (GPa) | $\Delta T_{max}(^0C)$ | s ($\mu$m) | # of cycles | $\sigma_u$ (MPa) |
|---|---|---|---|---|---|
| 212 | 106 (114) | 30 | 175 (127) | $10^8$ | 427 |
| 220 | 116 | 29 | 248 | $7.6 \times 10^5$ | |
| 240 | 105 | 44 | 201 | $3.0 \times 10^5$ | |
| 260 | 109 | 29 | 361 | $1.5 \times 10^5$ | |
| 280 | 104 | 44 | 308 | $6.9 \times 10^4$ | |

### R=0.5

| $\sigma_{max}$ (MPa) | $\overline{E}_{min}$ (GPa) | $\Delta T_{max}(^0C)$ | s ($\mu$m) | # of cycles | $\sigma_u$ (MPa) |
|---|---|---|---|---|---|
| 220 | 103 (95) | 6 | 162 (114) | $10^8$ | 478 |
| 240 | 101 (100) | 14 | 149 (122) | $10^8$ | 406 |
| 260 | 94 | 35 | 163 | $1.0 \times 10^6$ | |

16

| 270 | 97 | 21 | 182 | $8.7 \times 10^5$ |
| 280 | 96 | 14 | 146 | $5.1 \times 10^5$ |

(values in parenthesis relate to the residual strength test)

## Table II: Composite properties

| | |
|---|---|
| $E_f$ (GPa) | 200 |
| $E_m$ (GPa) | 98 |
| $r$ ($\mu$m) | 7.5 |
| $\upsilon_f$ | 0.35 |

## Table III: Values of $\tau$ calculated from hysteresis modulus, $\overline{E}$ (200 Hz)

$R=0.05$

| $\sigma_{max}$ (MPa) | # of cycles | $\tau$ (MPa) |
|---|---|---|
| 212 | $10^8$ | 11.7 (15.0) |
| 220 | $7.6 \times 10^5$ | 12.7 |
| 240 | $3.0 \times 10^5$ | 9.2 |
| 260 | $1.5 \times 10^5$ | 7.0 |
| 280 | $6.9 \times 10^4$ | 7.1 |

17

$$R=0.5$$

| | | |
|---|---|---|
| 220 | $10^8$ | 10.0 (7.7) |
| 240 | $10^8$ | 11.0 (9.2) |
| 260 | $1.0 \times 10^6$ | 8.4 |
| 270 | $8.7 \times 10^5$ | 8.7 |
| 280 | $5.1 \times 10^5$ | 10.9 |

(values in parenthesis were computed from $\overline{E}$ obtained from the residual strength tests)

**References**

[1] L.M. Butkus , L.P. Zawada and G.A. Hartman, "Room Temperature Tensile and Fatigue Properties of Silicon-Carbide Fiber-Reinforced Ceramic Matrix Composites," Aeromat '90, Advanced Aerospace Materials/Processes Conference, 21-24 May 1990, Long Beach, California (1990).

[2] J.W. Holmes and B.F. Sorensen, "Fatigue Behavior of Continous-Fiber Reinforced Ceramic Matrix Composites," in High Temperature Mechanical Behavior of Ceramic

Matrix Composites. Edited by S.V. Nair and K. Jakus. Butterworth-Hinemann, Boston, MA, 261-326 (1995).

[3] B.F. Sorensen, J.W. Holmes and E.L. Vanswijgenhoven, "Does a True Fatigue Limit Exist for Continuous Fiber-Reinforced Ceramic Matrix Composites?", *J. Am. Ceram. Soc.*, submitted (1998).

[4] D. Rouby and P. Reynaud, "Fatigue Behavior Related to the Interface Modification during Load Cycling in Ceramic-Matrix Composites, " *Comp. Sci. Techn.*, **48**, 109-118 (1993).

[5] A.G. Evans, F.W. Zok and R.M. McMeeking, "Fatigue of Ceramic Matrix Composites," *Acta Metall. Mater.*, **43**, 859-75 (1995).

[6] J.W. Holmes and C.Cho, "Experimental Observations of Frictional Heating in Fiber-Reinforced Ceramics," *J.. Am. Ceram. Soc.*, **75**, 929-38 (1992).

[7] S.F. Shuler, J.W. Holmes, X.Wu and D. Roach, "Influence of Loading Frequency on the Room-Temperature Fatigue of a Carbon-Fiber / SiC-Matrix Composite," *J. Am. Ceram. Soc.*, **76**, 2327-36 (1993).

[8] W. Morris, B.N. Cox, D. B. Marshall, R. Inman and M. James, "Fatigue Mechanisms in Graphite / SiC Composites at Room and High Temperature," *J. Am. Ceram. Soc.*, **77**, 792-800 (1994).

[9] A.G. Evans amd F. W. Zok, "The Physics and Mechanics of Fibre-Reinforced Brittle Matrix Composites," *J. Mater. Sci.*, **29**, 3857-96 (1994).

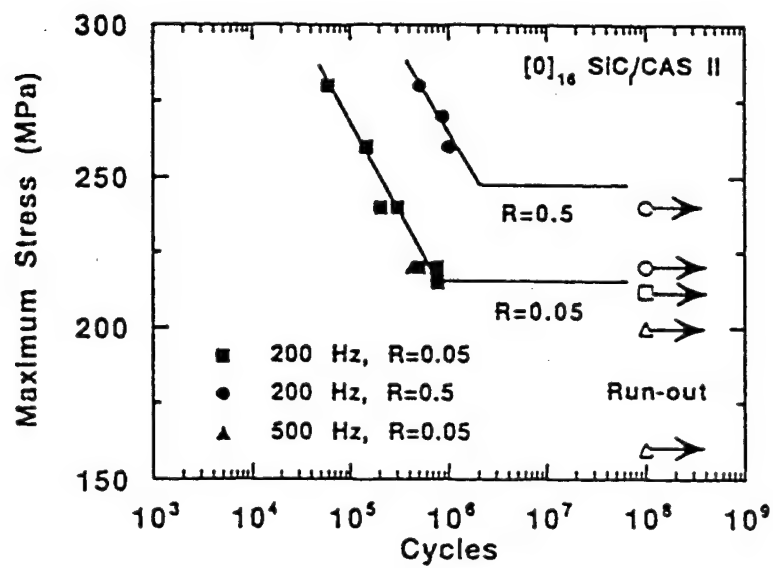[10] B.F. Sorensen, J.W. Holmes and E.L. Vanswijgenhoven, "Rate of Strength Decrease of Fiber-Reinforced Ceramic Matrix Composites during Fatigue," *J. Am. Ceram. Soc.*, submitted (1998).

[11] W.A. Thomas and J.M. Sanchez, "Influence of Interfacial Sliding Stress on Fatigue Behavior of Oxidized Nicalon / Calcium Aluminosilicate Composites," *J. Am. Ceram. Soc.,* **79**, 2659-65 (1996).

[12] F.E. Heredia, J.C. McNulty, F.W. Zok and A.G. Evans, "Oxidation Embrittlement Probe for Ceramic-Matrix Composites," *J. Am. Ceram. Soc.,* **78**, 2097-100 (1995).

[13] A.G. Evans, F.W. Zok, R.M. McMeeking and Z.Z. Du, "Models of High-Temperature, Environmentally Assisted Embrittlement in Ceramic Matrix Composites," *J. Am. Ceram. Soc., 79, 2345-52 (1996).*

[14] W.R. Moschelle, "Load Ratio Effects on the Fatigue Behavior of Silicon Carbide Fiber Reinforced Silicon Carbide Composite," *Ceram. Eng. Sci. Proc.* **15**, 13-22 (1994).

[15] J.W. Holmes, "Influence of Stress Ratio on the Elevated-Temperature Fatigue of Silicon Carbide Fiber-Reinforced Silicon Nitride Composite," *J. Am. Ceram. Soc.,* **74**, 1639-45 (1991).

[16] C. Cho, J.W. Holmes and J.R. Barber, "Estimation of Interfacial Shear in Ceramic Composites from Frictional Heating Measurements," *J. Am. Ceram. Soc.,* **74**, 2808-18 (1991).

[17] W.A. Curtin, "Theory of Mechanical Properties of Ceramic Matrix Composites," *J. Am. Ceram. Soc.,* **74**, 2837-45 (1991).

[18] I.M. Daniel, G. Anastassopoulos and J. –W. Lee, 1990, "Experimental Micro-Mechanics of Brittle-Matrix Composites," in Micromechanics: Experimental Techniques, AMD Vol. 102, (ed. Sharpe, W.N. jr.), American Society of Mechanical Engineers, New York, U.S.A., 133-46 (1990).
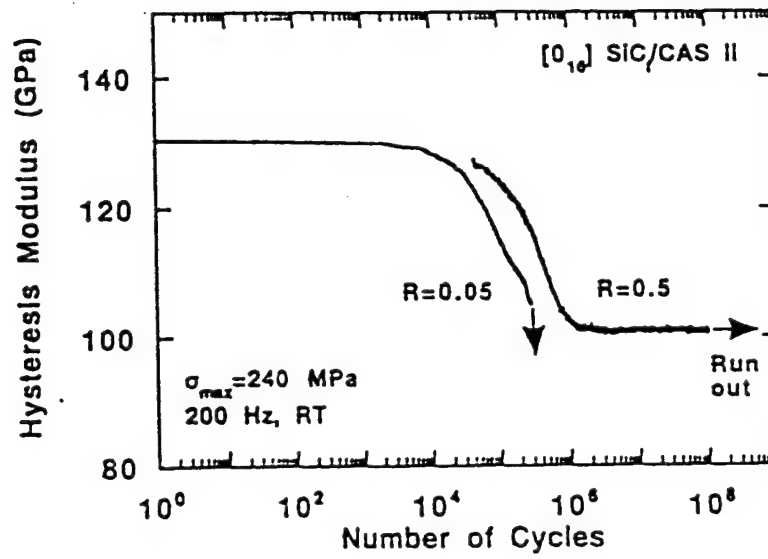
[19] A.W. Pryce and P.A. Smith, "Matrix Cracking in Unidirectional Ceramic Matrix Composites under Quasi-Static and Cyclic Loading," *Acta Metall. Mater.*,**41**, 1269-81 (1993).

[20] W.P. Keith and K.T. Kedward, "The Stress-Strain Behavior of a Porous Unidirectional Ceramic Matrix Composite," *Composites*, **26**, 163-74 (1995).

[21] B.F. Sorensen and J.W. Holmes, "Model of the Mechanical Behavior of Continous Fiber-Reinforced Ceramic Matrix Composites," manuscript in preparation.

[22] E. Lara-Curzio and M.K. Feber, "Methodology for the Determination of the Interfacial Properties of Brittle Matrix Composites," *J. Mater. Sci.,* **29**, 6152-8 (1994).

[23] S.M. Spearing, F.W. Zok and A.G. Evans, "Stress Corrosion Cracking in a Unidirectional Ceramic-Matrix Composite," *J. Am. Ceram. Soc.,* **77**, 562-70 (1994).

[24] A.G. Evans, "Design and Life Prediction Issues for High-Temperature Engineering Ceramics and Their Composites," *Acta Mater.* **45**, 23-40 (1997).
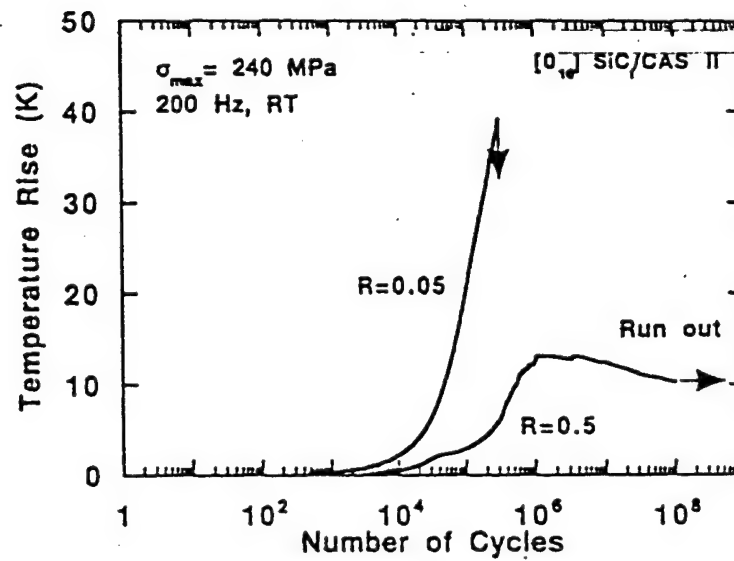
14.0   3.0 ，ɔminal)

8°±2'

39.3
(radius center)

18.1

R 152.4

6.3

111.7

1.3±0.1

7.0±0.1

1)   Geometry of the edge loaded tensile specimens used in the present study.

2) The S-N curve (relationship between the maximum applied stress and the number of cycles to failure) for $R = 0.05$ and $R = 0.5$. Both fatigue life and the fatigue limit (defined as run-out for $10^8$ cycles) increases with increasing stress ratio ( $\sigma_{max} = 240$ MPa).
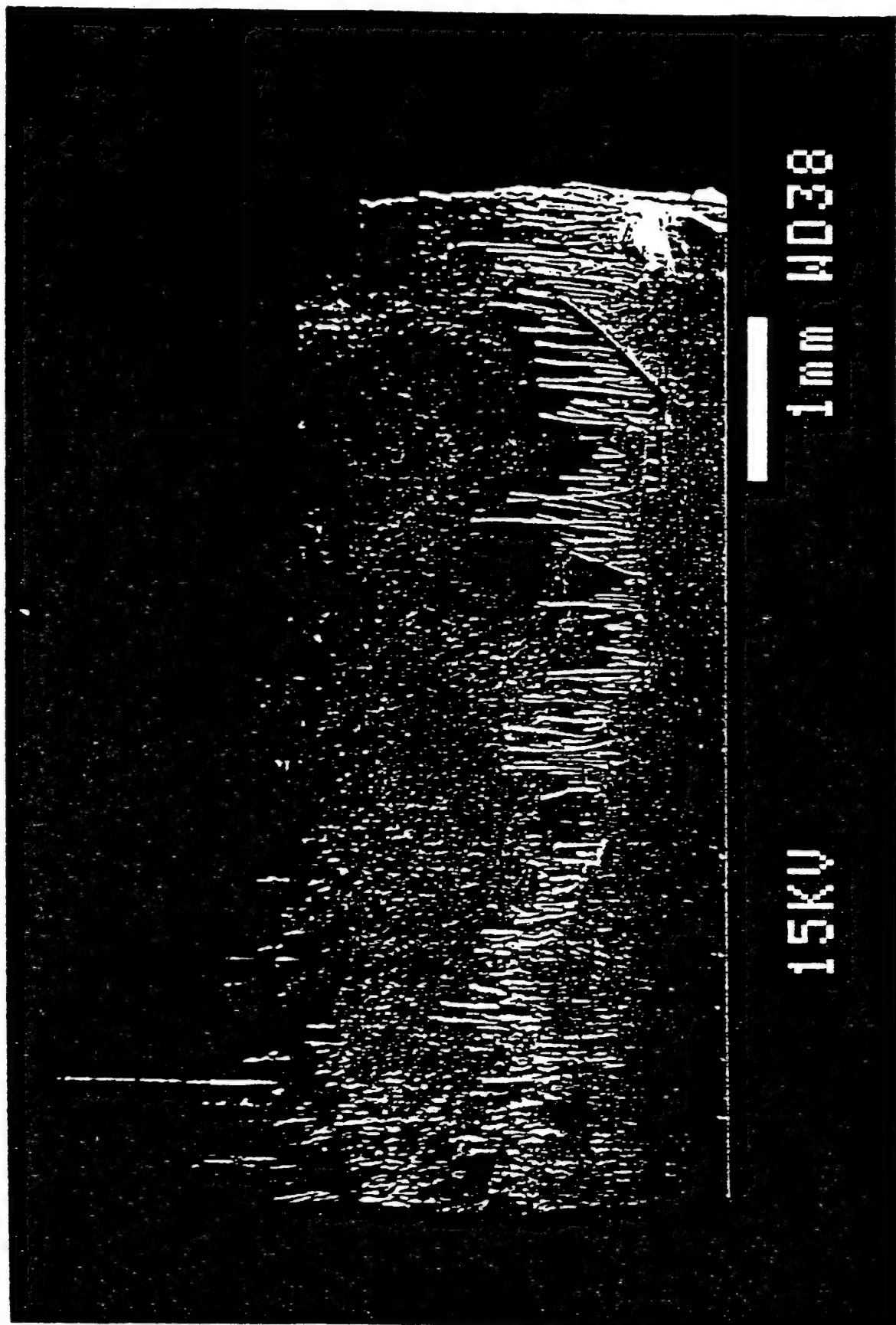
3)    Hysteresis modulus as a number of cycles for two specimens loaded with identical

maximum stress (240 MPa) at two stress ratios ($R = 0.05$ and $R = 0.5$).
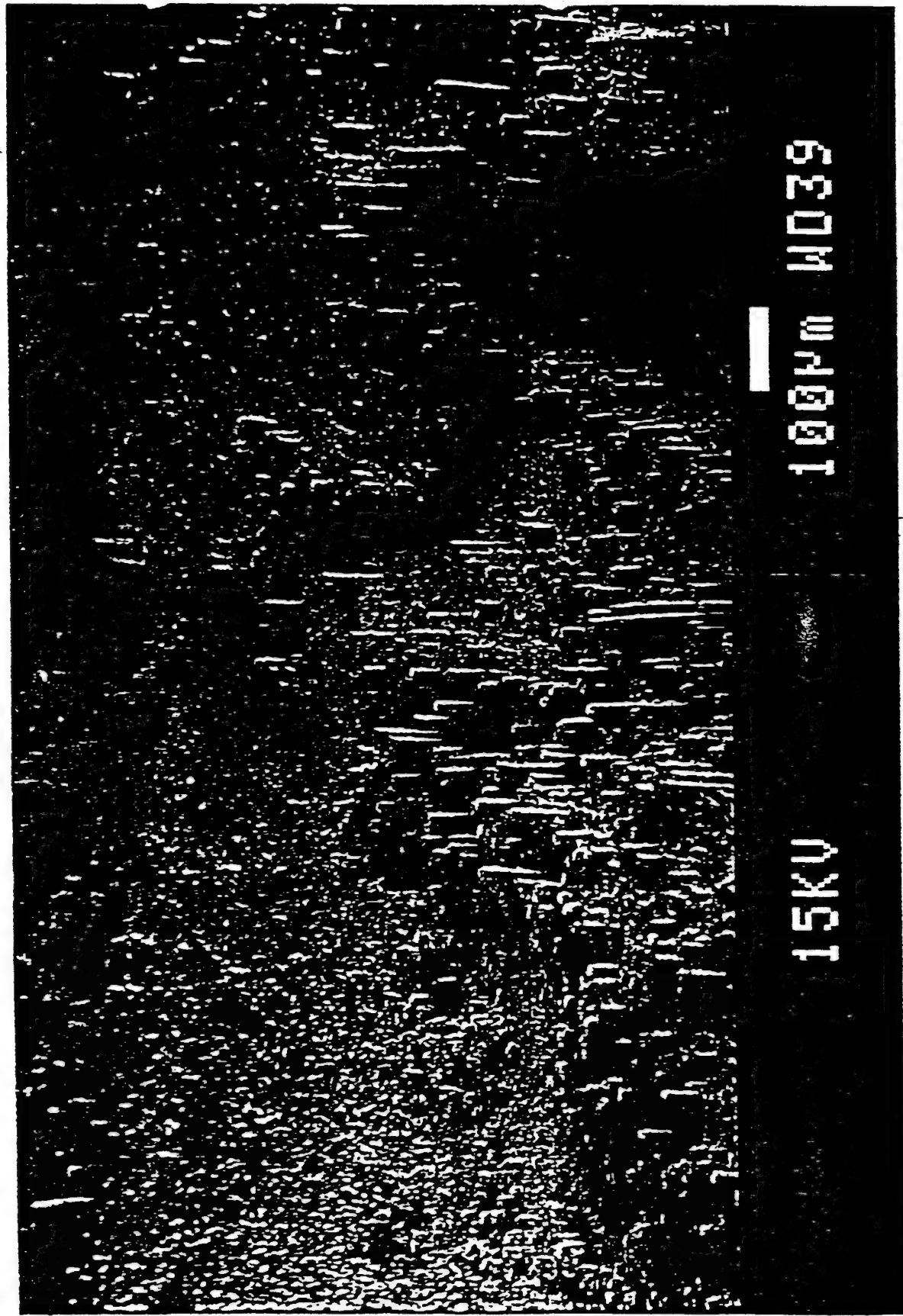
Figure showing Temperature Rise (K) vs Number of Cycles. $\sigma_{max} = 240$ MPa, 200 Hz, RT, $[0_{16}]$ SiC/CAS II. Curves for R=0.05 and R=0.5, with "Run out" indicated.

4)    The evolution of temperature rise of cyclically loaded specimens. The maximum

stress is identical for the two specimens (240 MPa), but their stress ratios are

different ($R = 0.05$ and $R = 0.5$)

5) Micrographs of fracture surface of a specimen failing in fatigue. (a) overview of fracture surface

(b) the transition zone between the central zone with (right) and

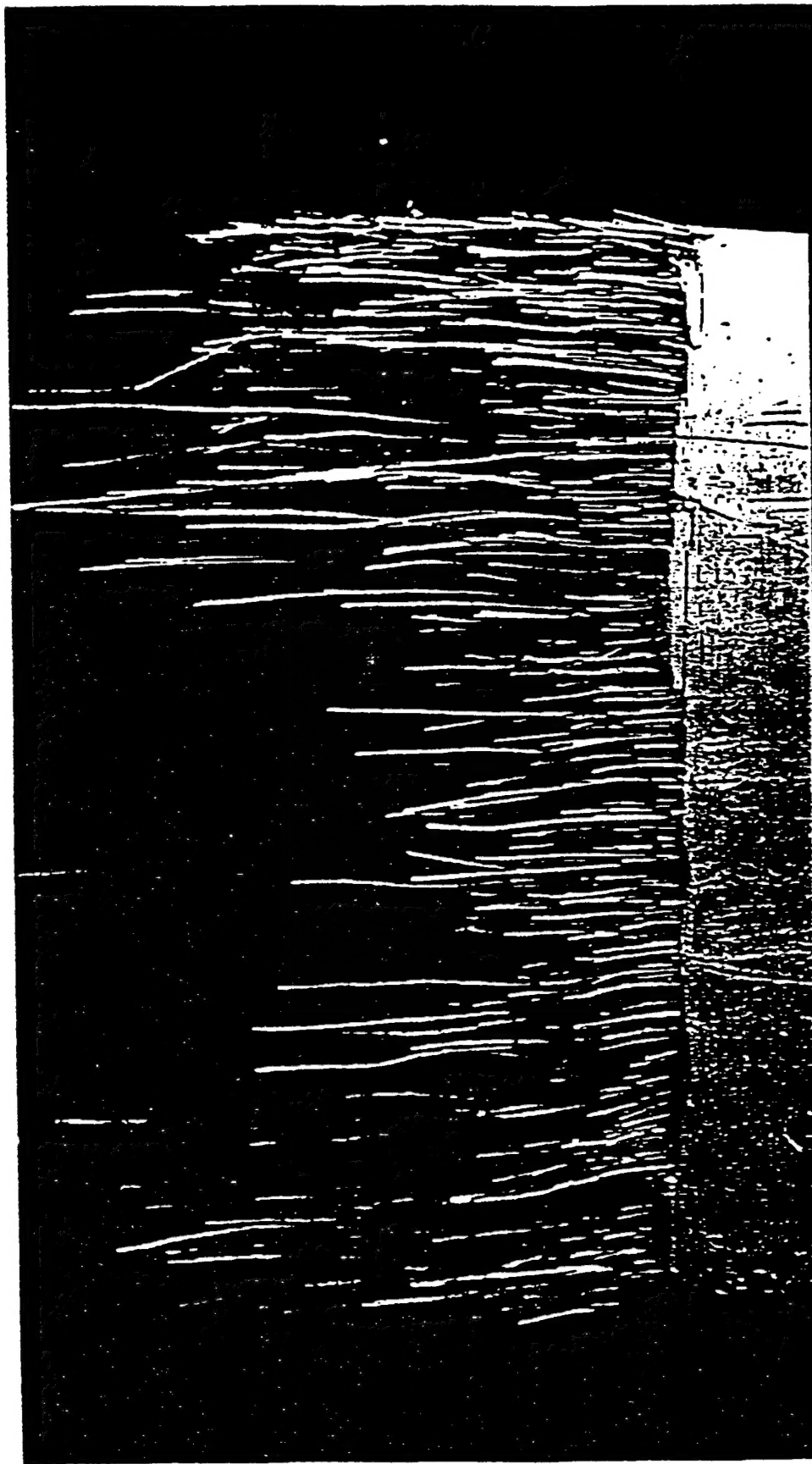without fiber pull out (left)

(c) close up of the central part of the fracture surface.

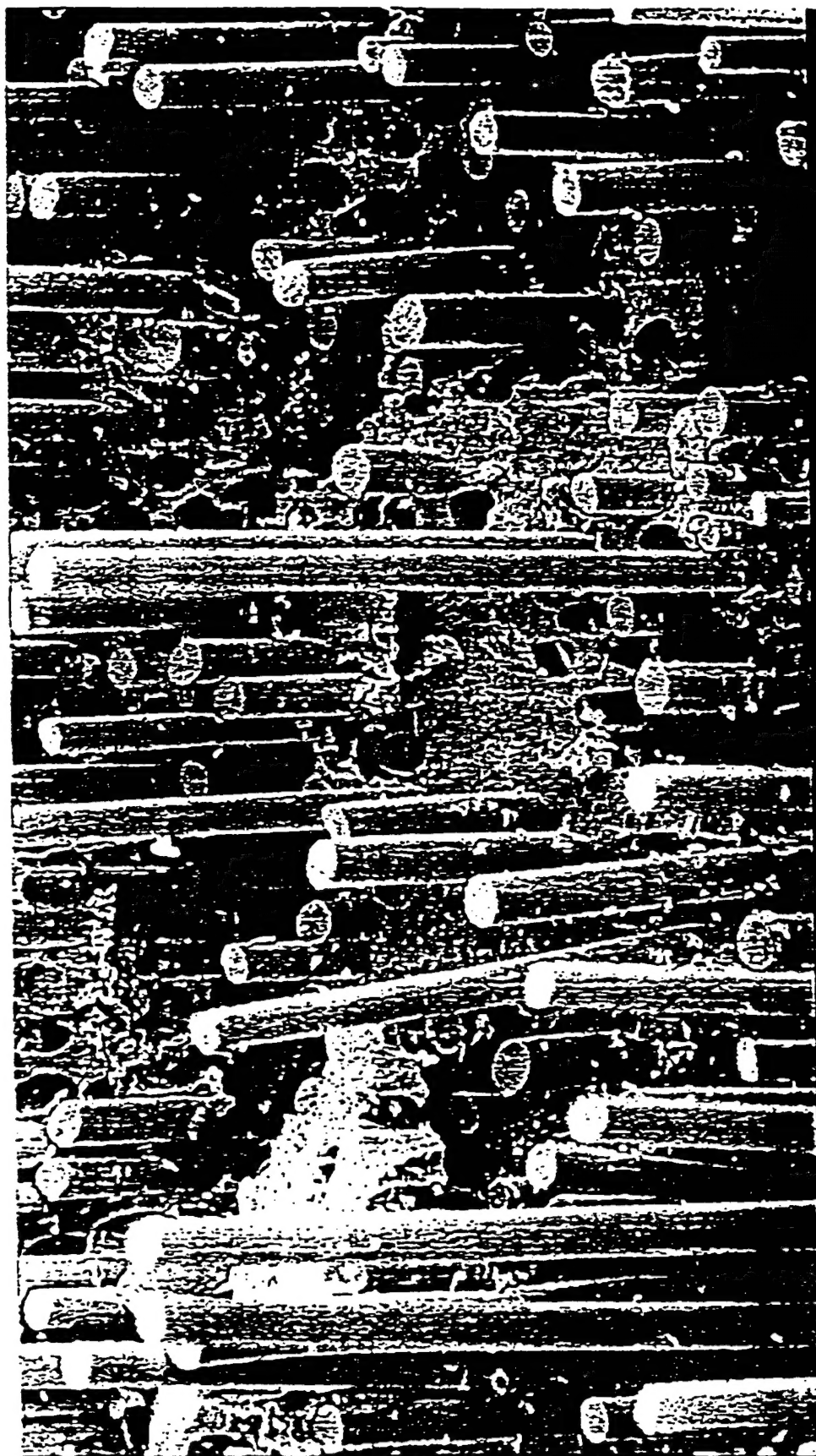Micrographs of fracture surface of a specimen that survived $10^n$ cycles. (a) overview

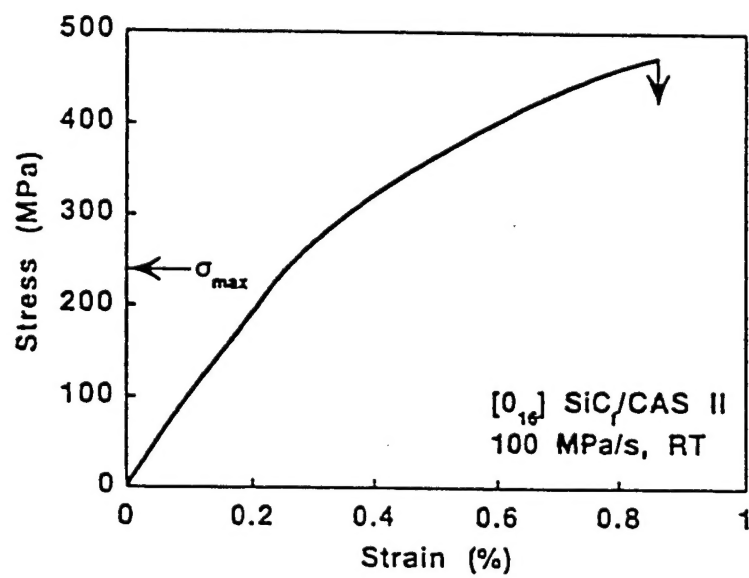(b) close up of the central part of the fracture surface.

Stress-strain curve showing Stress (MPa) versus Strain (%) for [0_{16}] SiC_f/CAS II at 100 MPa/s, RT, with σ_max marked.

7)      A typical stress-strain curve of a specimen after $10^8$ load cycles.